DFT and tight binding Monte Carlo calculations of single-walled carbon nanotube nucleation and growth

Wuming Zhu[1*], Anders Börjesson[1,2], My name[1,3], and Kim Bolton[1,2]

[1]*Physics Department, Göteborg University, SE-412 96, Göteborg, Sweden*

[2]*School of Engineering, University College of Borås, SE-501 90, Borås, Sweden*

[3]*Department of XXX, University of XXX, Zip code, City, Country*

(Dated: Jan 17, 2009)

Abstract

Density functional theory (DFT) calculations of the nucleation of $(5,5)$ and $(10,0)$ single-walled carbon nanotubes (SWNTs) on a 55 atom nickel cluster (Ni_{55}) showed that it requires a larger chemical potential to grow a carbon island (which is the precursor to the SWNTs) on the cluster than to extend the island into a SWNT or to have the carbon atoms dispersed on the cluster surface. Hence, in the thermodynamic limit the island will only form once the (surface of the) cluster is saturated with carbon, and the island will spontaneously form a SWNT at the chemical potentials required to create the island. The DFT (zero Kelvin) and tight binding Monte Carlo (1000 K) also show that there is a minimum cluster size required to support SWNT growth, and that this cluster size can be used to control the diameter, but probably not the chirality, of the SWNT at temperatures relevant to carbon nanotube growth. It also imposes a minimum size of clusters that are used in SWNT regrowth.

* Electronic address: wuming@lct.jussieu.fr
present address: Laboratoire de Chimie Théorique, UPMC Univ Paris 06, 75005 Paris, France.

1. INTRODUCTION

Chirality controlled growth of single-walled carbon nanotubes (SWNTs) is a hotly pursued goal since the SWNT chirality determines its electronic properties [1, 2]. The catalytic chemical vapor deposition (CCVD) method is favored for chiral-selective growth since it is more controllable than arc-discharge or laser-ablation. The CCVD parameters that have been adjusted and examined for controlling SWNT growth include the catalyst preparation and support, type of carbon feedstock, gas pressure and reaction temperature [3–12]. Although chiral selective growth has not been achieved, it is clear that changing these growth parameters affects reaction kinetics and(or) leads to preferential growth of a subset of SWNT chiralities [11]. In fact, a common result for most studies is that the catalyst particle composition and size is of central importance in SWNT production.

The linear correlation between the SWNT diameter and the size of the catalyst metal particle from which it grows has long been identified [13], with the ratio of the catalyst:SWNT diameters ranging from 1.1 to 1.6 [5, 6, 14]. Although there are several computational studies on cap nucleation [15–20], it is still debatable as to whether the catalyst particle determines the SWNT diameter at the nucleation stage (by providing a template for cap formation), or whether the SWNT changes diameter after nucleation to fit to the particle diameter. The relative importance of these two mechanisms may depend on the growth conditions and possible changes in the particle size during growth.

Calculations of cap formation energies on a rigid Ni(111) surface has also led to the suggestion of chiral-selective nucleation [18, 21]. This selectivity relies on epitaxial matching between the SWNT end and the Ni surface atoms, which are assumed to be immobile. However, the energies of the caps required for different SWNT chiralities differ by only a couple of eVs, and often not more than a few tenths of an eV. This, together with the fact that the high growth temperatures required for catalytic feedstock dissociation and carbon diffusion on the catalyst particle (the lowest diffusion barrier on Ni surfaces is 0.4 eV [22, 23]) are expected to lead to surface or bulk melting of the catalyst particle, places a severe limitation on the possibility of chiral-selective nucleation based on epitaxial matching between the SWNT and catalyst particle. In fact, in situ observations of CCVD carbon nanotube growth have shown that the Ni catalyst particle changes shape during growth even at low temperatures [24].

It is clear that SWNT nucleation and growth is a very complex process that requires further studies to deepen our understanding as well as to identify the extent that we can control the SWNT diameter and chirality. In this contribution we use DFT (at zero Kelvin) and tight binding based Monte Carlo (TBMC at 1000 K) to study the relationship between the catalyst particle size and the SWNT diameter and chirality. We focus on the $(5,5)$ and $(10,0)$ SWNTs and study their relative nucleation energies, as well as investigating the minimum particle size that is needed to support SWNT nucleation and growth. This is important for an increased understanding of the fundamental physical principles that control these processes, which is vital to develop strategies to engineer catalyst particles for controlled SWNT production. For example, we address the chemical potentials that are required at different stages in the SWNT nucleation, as well as the relative energies associated with growing the $(5,5)$ and $(10,0)$ SWNTs. This work also sheds light on the limitations of the CCVD method for chiral selective growth, and if these limitations cannot be overcome then other ways to achieve chiral selective growth or separation will need to be identified.

This work also addresses the minimum particle size that is required for SWNT regrowth, or seeded SWNT growth, which has been advocated for growing SWNTs with a specific chirarlity [25, 26]. In this method catalyst particles are docked onto existing SWNT seeds before extending the length of the seeds, with the aim that the newly grown regions of the SWNTs adopt the chirality of a parent seed. This complements our previous calculations which showed that thin SWNTs on a large Ni catalyst particle might increase their diameter during growth [27], which puts an upper limit to the proper particle size for growing thin SWNTs. In this contribution we investigate if there is a lower limit on the size of the particle needed for regrowth. We focus on metal particles that are gently docked on the SWNT end, although we have shown that the docking procedure is unlikely to affect the possibility for chirality controlled regrowth[28].

2. COMPUTATIONAL METHODS

2.1. Density functional theory calculation

The total energy DFT calculations were done using the VASP code [29, 30]. The generalized gradient approximation as in Perdew-Wang functional (PW91) [31] was used for the electron exchange-correlation energy, the nickel and carbon core electrons were treated using ultrasoft pseudopotentials, and the cutoff energy of the plane-wave basis set for expanding valence electrons was 286.7eV. Supercell sizes were sufficiently large to allow for single Γ-point k-space sampling. All calculations were spin-polarized except mentioned otherwise. Total energies converged to 1 meV. These methods and parameters have been successfully used in previous studies of SWNT/Ni systems[27, 32].

As mentioned earlier, this study focuses on carbon/nickel systems of relevance to SWNT nucleation and growth. We focus on $(5,5)$ and $(10,0)$ SWNTs, and investigate clusters of different sizes. The initial structure of the clusters were obtained by cutting from the bulk fcc structure. The cluster and the SWNT/metal structures were fully relaxed by a conjugate-gradient (CG) algorithm without symmetry constraint. Although the structures obtained by this method are not expected to be the global minimum, the trends reported here are expected to be correct. This is supported by the fact that the TBMC method (at 1000 K) was also used to obtain annealed starting structures for the DFT calculations, and the energies obtained from these structures are in close agreement with those obtained from the fcc structures.

In order to compare systems with different numbers of Ni and carbon (C) atoms we use the free Ni cluster and C atoms in an infinite graphene sheet as references for expressing the system total energy. This has previously been used to study the relative stability of different caps on Ni surfaces [16, 18]. Hence, the total energy is

$$E_{tot} = E(C/Ni_{cluster}) - E(Ni_{cluster}) - n_C E_{graph} \quad (1)$$

where $E(C/Ni_{cluster})$ is the energy of the C/Ni system, $E(Ni_{cluster})$ is the energy of the isolated (and re-optimised) Ni cluster, n_C is the number of carbon atoms, and E_{graph} for the energy of the infinite graphene sheet per C atom. Since all of the energies on the right hand side of Eq. (1) are negative, a larger positive value of E_{tot} reflects an increasing instability of the C/Ni system. It is important to note that E_{graph} is a constant value, so that using

a different reference (e.g., carbon gas) would yield a different constant value and will not change the trends and results reported here.

Eq. (1) can be reformulated in terms of the chemical potential with respect to graphene, μ, which is the energy required to add a carbon atom at different stages of the SWNT nucleation. That is,

$$\mu = dE_{tot}/dn_C \tag{2}$$

where dE_{tot} is the change of total energy when adding dn_C carbon atoms to the system but keeping the number of Ni atoms unchanged. Remember that $n_C E_{graph}$ has already been subtracted out in Eq. (1).

Another energy that is often used in theoretical studies of SWNT growth, and that we will also use here, is the binding (or adhesion) energy. Here the isolated (and re-optimised) carbon and Ni structures are the references, i.e.,

$$E_b = E(C/Ni_{cluster}) - E(Ni_{cluster}) - E(C_{structure}) \tag{3}$$

where $E(C_{structure})$ is the energy of the isolated carbon structure. In the case that the system contains only one carbon atom, this is the energy of the triplet state. A negative E_b shows that the C/Ni system is more stable than the separated metal and carbon systems.

DFT based molecular dynamics (MD) simulations were performed for the (5,5) SWNT cap attached to the Ni_{55} cluster in order to elucidate finite-temperature effects. Only a single short trajectory (3.75 ps) was propagated due to the computational expense of this method. To increase the computational efficiency we used local density approximation (LDA) for the exchange-correlation, and valence electrons were treated as non spin-polarized. The integration time step was 1 fs, and the temperature was raised from 0K to 1000K over 1.75 ps before maintaining a constant temperature (1000 K) for 2 ps. The similarity of the results found from these simulations compared to the zero Kelvin DFT calculations and 1000 K TBMC supports the validity of this method.

2.2. Tight binding Monte Carlo

The semiempirical studies are based on a fourth moment tight binding approximation combined with canonical MC [33, 34]. This method complements the DFT calculations since it allows simulations at finite temperatures with good statistics. All data are obtained

after performing a minimum of $60000N_{tot}$ MC displacements, where N_{tot} is the total number of atoms, to ensure equilibration (seen by constant average properties).

3. RESULTS AND DISCUSSION

The Ni_{55} cluster was initially used to study the formation of (10,0) and (5,5) SWNT caps. As illustrated in Fig. 1 (c-d), these caps fit the five-fold symmetry of the free Ni_{55} cluster.

The most stable adsorption site for a single C atom is on the edge of the fcc Ni structure (see Fig. 1(a)), which provides 5 neighboring Ni atoms. The binding energy is -7.5 eV. This is a slightly stronger bond than that determined with the same functional and code for a (111) surface of a Ni_{38} cluster, which is -7.2 eV [35]. The total energy, E_{tot}, for 1 C adsorbed on Ni_{55} (Fig. 1(a)) is 0.38 eV. It may be noted that adsorption at subsurface sites may be more stable[36, 37]. This was not investigated further here, and does not affect the conclusions presented below. Hence, the chemical potential for the first C atom on a Ni_{55} cluster is $\mu_{1C} = 0.38$eV (i.e., the carbon atom would rather be in a graphene sheet than on the surface of the cluster).

The simplest structure (island) that can lead to the formation of (10,0) and (5,5) SWNTs is shown in Fig 1(b). This island consists of 20 C atoms and has one pentagon surrounded by five hexagons. The total energy of this island is 16.8 eV, which yields a chemical potential of 0.84 eV/C. This is higher than the chemical potential for the single carbon atom discussed above (0.38 eV) which shows that C atoms at low coverage will not spontaneously nucleate an island. This is consistent with molecular dynamics and Monte Carlo simulations of SWNT growth[36, 38, 39]. Spontaneous nucleation of the island requires a large surface coverage which, in its turn, requires a chemical potential in excess of 0.84 eV/C.

Given that one has a sufficiently high chemical potential (i.e., a sufficiently high carbon feedstock pressure in CCVD growth) to form the island in Fig. 1(b), it is possible to form the (10,0) or (5,5) SWNT, as shown in Fig. 1(c) and (d). As shown in the figure, the total energy of the (10,0) cap is 1.6 eV higher than that of the (5,5) cap. This is similar to the energy difference (1.1 eV) on a Ni(111) surface obtained previously [18]. The chemical potentials for the carbon atoms that are added to the island structure (i.e., to grow the island in Fig. 1(b) into the caps in Fig. 1(c) and (d)) are 0.01 eV/C and -0.07 eV/C for the (10,0) and (5,5) SWNT caps, respectively. Both of these are lower than 0.84 eV/C to form the island

in Fig. 1(b) and $\mu_{1C} = 0.38$ eV for the adsorption of isolated carbon atoms on the cluster, which shows that the growth of the SWNT caps from the island is spontaneous and that the island (and SWNT caps) drains C atoms adsorbed on the cluster, thereby inhibiting the formation of extra islands on the particle provided that C atoms can readily diffuse to the island edge. This is in agreement with MD simulations [39] and explains why small catalyst clusters produce only one SWNT [40]. It is important to note that our results do not indicate that there are no isolated carbon atoms on the cluster during SWNT growth, since we have not investigated the intermediate growth steps. That is, systems that have incomplete rings at the SWNT end are expected to have higher chemical potentials than those obtained here. This is supported by preliminary results obtained by the TBMC simulations which show that SWNTs that end with incomplete rings are more prone to dissolve into the Ni cluster than SWNTs that end with complete rings.

It may be noted that the island in Fig. 1(b) includes one pentagon, whereas any complete cap has 5 more pentagons. Since a pentagon has 5 sides, its formation can be facilitated at vertices of catalyst particles that have 5-fold symmetry, such as that in Fig. 1. In contrast, flat and perfect surfaces cannot have 5-fold symmetry and hence are less suitable for SWNT growth. Of importance to this work is that a larger chemical potential is required to nucleate the island in Fig. 1(b) than to extend this island into (10,0) or (5,5) SWNTs. Since the same island forms both chiralities, and since the extension of the island to both SWNTs is spontaneous, one cannot control which of these SWNTs is formed from this island.

During structure optimizations, we observed the rotation of the island or caps relative to the Ni cluster, and reshaping of the cluster. This is because the Ni atoms at the edge of the island or cap are more strongly bonded to the edge C atoms than the surrounding nickel atoms. This means that the edge C atoms determine the positions of bonded Ni atoms, and hence the cluster shape adapts to the shape of the island or cap edge (and not vice versa). The ability of the metal clusters to adapt their shape to evolving SWNT edge configurations during growth prevents the formation of dangling C bonds.

The ability of the cluster to adapt its shape to the structure of the SWNT cap edge (and not vice versa) as well as the stability of the cap was also observed in the DFT MD simulations of the (5,5) cap on the Ni_{55} cluster at 1000 K. The Ni cluster adjusts its shape to fit to the cap structure by becoming flatter, especially at the side of the (5,5) cap. Also, none of the carbon atoms dissociate from the cap during simulation. This, together with

the fact that previous simulations showed that carbon atoms on Co cluster surfaces diffuse to, and are captured by, the cap edge [15] support the conclusion that the cap acts as a sink for isolated carbon atoms.

Fig. 1 shows the scenario where the island (panel (b)) grows into SWNT caps. However, it is also possible that this island merely grows in size, e.g., by adding only hexagons instead of pentagons to the island. Extending the island by a ring of 10 hexagons (figure not shown) yields a larger island with 45 C atoms. Its total energy is 25.6 eV, which yields a chemical potential for the additional carbon atoms of 0.35 eV/C. This is lower than the chemical potential required to build the island (0.84 eV/C) which means that the island is spontaneously extended once it it formed. However, it is far larger than the chemical potentials to extend the island into the (10,0) and (5,5) SWNT caps (0.01 eV/C and -0.07 eV/C, respectively), so that cap formation is preferred.

From the above discussions it is clear that the Ni_{55} cluster preferentially grows (5,5) and (10,0) SWNTs and not nanotubes with larger diameters, but there is not a strong preference for one of the chiralities. That is, for the island in Fig. 1(b), cap formation is strongly favored over island size-extension, so it is unlikely that SWNTs with diameters larger than 10Åare grown from Ni_{55}. However, the (10,0) and (5,5) caps have very similar energies, with a difference in the chemical potentials of the edge atoms of only 0.08 eV/C. This is similar to the thermal energy of atoms at typical growth temperatures, and is much smaller than the C diffusion barriers on the Ni surface [22, 23]. (Note that activation barriers for formation of the different caps have not been studied, which is beyond the scope of this work.) Hence, it appears that the cluster plays a significant role in determining the SWNT diameter, but cluster engineering alone does not seem to be a promising method for chirality controlled SWNT production.

Smalley et al. proposed SWNT regrowth as a method for chirality controlled mass production of SWNTs [25, 26]. This approach avoids the cap nucleation step which, as discussed above, is expected to lead to the formation of SWNTs that have a variety of chiralities. Instead, existing SWNTs are used as seeds for further growth. This is achieved by cutting the seed SWNTs to expose their ends, and then docking metal catalysts on these ends before introducing carbon feedstock for continued growth. In a recent study that uses the TBMC method discussed above, we showed that the seed SWNT preserves its structure for different catalyst docking methods[28], which indicates that the SWNT regrowth method may be a

robust method for chiral selective growth. In fact, in the regrowth experiments the catalyst clusters are formed by deposition of metal vapour in the apparatus (on the SWNTs, substrate, etc) and then heating so that the deposited vapour aggregates into clusters at the SWNT ends. In this study we examine the size of the cluster that is required for SWNT regrowth. In particular, we investigate the minimum size of the particle that is required for continued growth.

Our approach is to consider if a cluster of a certain size will maintain the open end of a seed SWNT, or if the SWNT prefers to form a cap with the catalyst particle adsorbed on the outside of the cap or separated from the SWNT. We start by considering a single Ni atom, which may be relatively mobile along SWNT open edges and which may also be capable of annealing carbon pentagons hence maintaining an open end [41]. The relevant structures for the (10,0) SWNT are the nanotube attached to the Ni atom and the fullerene also attached to the Ni atom. These structures are shown in Fig. 2(a) and (b). The total energies are 43.5 eV for the SWNT cap structure and 26.0 eV for the C_{80} I_h fullerene cage structure, showing a strong preference for the SWNT to close if only a single Ni atom is docked onto the open end.

This approach was extended to include Ni clusters containing 10, 25, 34, 43, 55 and 201 atoms. Clusters larger than 25 atoms were cut from the fcc Ni structure followed by relaxation without symmetry restriction. (10,0) SWNTs, (5,5) SWNTs, I_h C_{80} fullerenes and D_{5d} C_{80} fullerenes were then placed arbitrarily on the clusters before geometry optimization of the entire system. The final structures are not expected to be global minima, but finding global minima of large clusters from DFT calculations is not feasible [42]. To investigate possible errors associated with this approximation, a few final structures were used to initiate DFT-based MD simulations at 1000 K. No significant structural change was observed during these simulations. In addition, we used TBMC simulations (annealing from 1000 K) to obtain four different initial structures for the Ni_{25}, Ni_{34} and Ni_{43} systems. The final energies of the four DFT-relaxed configurations differ by as much as 2$\sim$3 eV, and were often lower in energy than the structure obtained from the fcc geometry. We present the results of the systems that have the lowest energies (see Fig. 3).

When each dangling bond at the open end of the (10,0) SWNT cap is attached to a Ni atom, as shown in Fig. 2(c), the total energy decreases from 49.5 eV to 31.2 eV. The Ni_{10} cluster adopts a pentagonal shape, which is not expected to be stable since it differs

significantly from that of the isolated minimum energy cluster. In fact, three isomers of the isolated Ni_{10} cluster are very close in energy[43], and we arbitrarily selected the tetragonal antiprism structure to attach to the open end of the (10,0) SWNT. Upon relaxation the Ni atoms are attracted to the dangling C bonds and none of the cluster atoms are located inside the SWNT cap (retraction of metal clusters from SWNTs is discussed in detail elsewhere [28]). As seen in Fig. 2(d), the SWNT cap is deformed since the cluster has a smaller diameter than the nanotube. In spite of this deformation, the total energy of this system (29.1 eV) is lower than that of the system containing the pentagonal formation of the Ni cluster (31.2 eV). However, this energy is 4.1 eV higher than that of the C_{80} I_h fullerene attached to the Ni_{10} cluster (Fig. 2(f)), which means that the Ni_{10} cluster is not expected to support regrowth of the (10,0) SWNT. Although we have not considered the effect of activation barriers that may hinder SWNT closure, we show that an intermediate structure for SWNT closure from Fig. 2(d) to 2(f), i.e., the unclosed cage structure C_{75} with the metal cluster at the aperture shown in Fig. 2(e), has an energy of 26.3 eV. Thus, it is probable that the (10,0) SWNT on the Ni_{10} will form a dome structure (Fig. 2(e)) and terminate its growth as shown in Fig. 2(d-f).

Fig. 3(a) shows the total energies of the Ni cluster systems that we have investigated, attached to a (5,5) SWNT cap (□), a (10,0) SWNT cap (△), a C_{80} D_{5d} fullerene (■) and a C_{80} I_h fullerene (▲). In contrast to the relatively constant energies of the C_{80} fullerene cage structures with change in particle size, the total energies of the (5,5) and (10,0) SWNT systems decrease with increasing cluster size (remember that this energy is relative to the isolated clusters and carbon atoms in a graphene sheet). This decrease in total energy is primarily due to the increase in SWNT/cluster binding (adhesion) energies with increasing cluster size. Since a strong SWNT/metal adhesion is necessary to keep the SWNT end open during growth [44], a sufficiently large metal catalyst particle is required for continued growth. In fact, it is clear from Fig. 3 that the Ni_{10} cluster (and perhaps even the Ni_{25} cluster) is not expected to support continued growth of either SWNT, since the energies of the fullerene structures are significantly lower than those of the SWNT structures.

We note that energies for the separated fullerene and cluster systems are not given in Fig. 3. The energies are typically 2∼3 eV higher than the energies shown in the figure (where the cluster is attached to the fullerene). Also, the reason for the non-monotonic decrease in the SWNT energies with increasing cluster size, as seen in Fig. 3(a), is not known, but

may be due to the fact that local energy minima were probably used in the calculations. In addition, the (10,0) SWNT systems have larger energies for small clusters than the (5,5) SWNT systems. This may be because the bonding between the (10,0) SWNT and the cluster is stronger than that between the (5,5) SWNT and the cluster [44], and this leads to a larger deformation of the cluster and SWNT for small clusters (and hence a higher total energy).

To analyze the correlation between the diameters of SWNT and catalyst particle, we define the diameter of the cluster as

$$D = \sqrt{20/3} R_g, \tag{4}$$

where R_g is the radius of gyration $R_g^2 = (1/N)\sum_I (R_I - R_{cm})^2$, and N is the number of metal atoms in the cluster. This definition yields diameters that are 2.5Å(the atomic distance in bulk Ni) smaller than those obtained in [45], because spreading of the electron density outside of the cluster is not included in this work. That is, we compare the diameters associated with the nuclei of the metal and carbon atoms. This is in consistent with the conventional definition of the SWNT diameter [2] and that is also used here, i.e.,

$$D_{SWNT} = \sqrt{3} a_{C-C} \sqrt{m^2 + mn + n^2}/\pi \tag{5}$$

for a (n, m) SWNT. Here a_{C-C} is the nearest-neighbor C-C distance. The diameters of (5,5) and (10,0) SWNTs are 6.9Åand 7.9Å, respectively.

To analyze the diameters it should be realized that D is the real diameter for a homogeneous spherical cluster, and that it increases with increasing deformation (e.g., flattening or elongation) of the cluster. The lower panel in Fig. 3 shows the diameters for isolated clusters (•), and when the cluster are attached to (5,5) and (10,0) SWNTs (□ and △, respectively). Since the deformation of the Ni_{10} clusters is large when they are docked on to the SWNT open ends (e.g., Fig. 2(d) for the (10,0) SWNT), their diameters are far larger than for the isolated cluster. There is also a noticeable difference between diameters of the free and docked Ni_{25} clusters. The difference diminishes with increasing particle size. This is consistent with the fact that small clusters cannot support continued SWNT growth since their deformation—as well as the deformation of the SWNT—yields total energies that are larger than those of the fullerene systems.

It is worthy to note that the diameter of free Ni_{25} is 7.7Å, very close to the diameters of (5,5) and (10,0) SWNTs (6.9Åand 7.9Å, respectively). However, as shown in Fig. 3,

the cluster deforms slightly when it attaches to the SWNT ends. In addition, the fullerene structures are energetically more favorable than (5,5) and (10,0) SWNT cap structures by 0.5 eV and 0.9 eV, respectively. This indicates that Ni_{25} may not support continued growth for either nanotube (partially due to the higher energy caused by the cluster deformation).

As discussed above, the validity of the DFT results were tested using TBMC simulations at 1000K, a typical temperature for CCVD SWNT growth. The system energies (i.e., the tight binding energies of the entire system) instead of the DFT total energies (as defined in Eq. (2)) were used for the present analysis, since the same number of metal and carbon atoms were used in each pair of SWNT/Ni_N and fullerene/Ni_N systems. The energy histograms, obtained from different configurations along the MC simulation, for clusters N = 10, 25, and 55 are presented in Fig. 4. Solid curves are for SWNT/Ni_N systems and dashed curves for the C_{80}/Ni_N systems. In agreement with the DFT results, the fullerene systems have lower energies than the SWNT systems for N = 10 and 25, whereas the SWNT systems are more stable than the fullerene systems for N = 55. Hence, in contrast to Ni_{10} and Ni_{25} clusters, a Ni_{55} cluster is expected to sustain regrowth of (10,0) and (5,5) SWNTs.

Both our DFT total energy calculations at 0K and TB simulations at elevated temperature indicate that the smallest Ni_N cluster for continuous growth of (5,5) and (10,0) SWNTs is N = 30$\sim$45 atoms, corresponding to D = 8.4$\sim$9.4Å. Thus, the lower limit of the ratio between diameters of catalyst particle to SWNT is 1.1$\sim$1.3, similar to the ratios of 1.1 to 1.6 that have been found experimentally [5, 6, 14]. However, the comparison should be cautioned because of different catalysts used in the experiments, the effect of catalyst supports, different methods used to measure the diameters and possible inaccuracies in DFT and TB models. Including reaction barriers may also modify the ratio determined from our thermodynamic calculations.

The lower limit of the ratio of the catalyst:SWNT diameters determined here does not exclude the possibility that larger catalyst particles can also sustain continued SWNT growth. The ratios of the catalyst and SWNT diameters at the nucleation stage and at the growth stage can also be different if the particle size changes, e.g., by sintering, evaporation or aggregation. Future studies need to address how the ratio depends on catalyst composition, temperature, supporting substrate, etc.

The largest Ni cluster we have investigated here is the Ni_{201} icosahedron. It has facets larger than the cross sections of (5,5) and (10,0) SWNTs, so the cluster essentially provides

an infinitely large Ni(111) surface to the tubes. Previously we suggested the possibility of thin ($D_{SWNT} < 5$Å) SWNTs increasing their diameter during growth if the Ni cluster is large compared to the nanotube [27]. The increase in the SWNT diameter lowers the system energy primarily due to a lowering in the curvature energy. This puts an upper limit to the catalyst particle size for continued growth of thin SWNTs. However, increasing diameter needs to introduce a heptagon at the growth edge, which is energetically more costly than introducing a pentagon. If the introduction of a heptagon is not accompanied by a sufficiently large decrease in curvature energy, it is less likely to occur. Hence, larger diameter SWNTs, such as those studied here, may not have an upper limit of the cluster size for continued growth. This may not be the case for SWNT nucleation (where large clusters may yield larger diameter nanotubes) and, from the results presented here, it is expected that seeded growth places less demands on controlling the cluster size.

4. SUMMARY AND CONCLUSIONS

DFT total energy calculations and TB simulations have been used to investigate and compare two routes toward diameter and chirality selective SWNT growth, i.e., nucleation of appropriate caps with the possibility for epitaxial matching with the catalyst cluster and seeded regrowth of SWNTs. The two routes have significantly different mechanisms to control SWNT diameter and chirality. While uniform sized catalyst particles can nucleate and grow SWNTs with a narrow diameter distribution, it seems incapable to grow SWNTs with a desired chirality in the absence of other SWNT chiralities. Creating the carbon island which is the precursor of the SWNT cap is energetic costly, and once this island is created its extension into a larger island or a SWNT cap is spontaneous. Hence, the island determines neither the diameter nor the chirality of the SWNT which eventually formed. However, extension of the island on the Ni_{55} particle studied here leads preferentially to the formation of SWNT caps, and not an increase in the size of the island, and in this way determines the diameter of the SWNT caps that are nucleated. In contrast, the energy difference when extending the island to form a (10,0) or a (5,5) SWNT cap is comparatively small and, neglecting the possible role of activation barriers in the growth, it is not expected that one can selectively grow caps with a desired chirality in the absence of other chiralities.

Seeded regrowth of SWNTs appears to offer a more robust route for chirality selective

growth. Our DFT and TBMC calculations show that the ratio of catalyst:SWNT diameters must be at least 1.1∼1.3 for the Ni particle to support continued SWNT growth. If the catalyst particle that is docked on to the SWNT open end is too small, the SWNT end closes and the growth terminates. This is in agreement with recent experimental studies of the effect of Ostwald ripening on SWNT growth[46], which indicate that catalyst particles do not support growth once they become too small. Only sufficiently large particles provide the strong carbon/metal adhesion that is required to maintain the open end of the growing nanotube. Although the cluster cannot be too large for the continued growth of thin SWNTs, this upper limit is not expected to be applicable to the larger diameter nanotubes that are typical grown via CCVD.

ACKNOWLEDGMENTS

The computations were performed on C3SE computing resources at the Chalmers University of Technology and at the Swedish National Supercomputing facilities. Financial support was obtained from the Swedish Research Council, the Swedish Foundation for Strategic Research (CARAMEL consortium) and the University of Gothenburg Nanoparticle Platform.

[1] Baughman RH, Zakhidov AA, de Heer WA. Carbon nanotubes–the route toward applications. Science 2002;297(5582):787–792.

[2] Dresselhaus MS, Dresselhaus G, Eklund PC. Science of fullerenes and carbon nanotubes. San Diego CA: Academic Press. 1996.

[3] Li Y, Kim W, Zhang Y, Rolandi M, Wang D, Dai H. Growth of single-walled carbon nanotubes from discrete catalytic nanoparticles of various sizes. J Phys Chem B 2001;105(46):11424–11431.

[4] Cheung CL, Kurtz A, Park H, Lieber CM. Diameter-controlled synthesis of carbon nanotubes. J Phys Chem B 2002;106(10):2429–2433.

[5] Kondo D, Sato S, Awano Y. Low-temperature synthesis of single-walled carbon nanotubes with a narrow diameter distribution using size-classified catalyst nanoparticles. Chem Phys Lett 2006;422(4-6):481–487.

[6] Inoue T, Gunjishima I, Okamoto A. Synthesis of diameter-controlled carbon nanotubes using centrifugally classified nanoparticle catalysts. Carbon 2007;45(11):2164–2170.

[7] Lu C, Liu J. Controlling the diameter of carbon nanotubes in chemical vapor deposition method by carbon feeding. J Phys Chem B 2006;110(41):20254–20257.

[8] Wang B, Poa CHP, Wei L, Li L-J, Yang Y, Chen Y. (n,m) selectivity of single-walled carbon nanotubes by different carbon precursors on Co-Mo catalysts. J Am Chem Soc 2007;129(29):9014–9019.

[9] Hiraoka T, Bandow S, Shinohara H, Iijima S. Control on the diameter of single-walled carbon nanotubes by changing the pressure in floating catalyst CVD. Carbon 2006;44(9):1853–1859.

[10] Ducati C, Alexandrou I, Chhowalla M, Amaratunga GAJ, Robertson J. Temperature selective growth of carbon nanotubes by chemical vapor deposition. J Appl Phys 2002;92(6):3299-3303.

[11] Bachilo SM, Balzano L, Herrera JE, Pompeo F, Resasco DE, Weisman RB. Narrow (n,m)-distribution of single-walled carbon nanotubes grown using a solid supported catalyst. J Am Chem Soc 2003;125(37):11186–11187.

[12] Lolli G, Zhang L, Balzano L, Sakulchaicharoen N, Tan Y, Resasco DE. Tailoring (n,m) structure of single-walled carbon nanotubes by modifying reaction conditions and the nature of the support of CoMo catalysts. J Phys Chem B 2006;110(5):2108–2115.

[13] Dai H, Rinzler AG, Nikolaev P, Thess A, Colbert DT, Smalley RE. Single-wall nanotubes produced by metal-catalyzed disproportionation of carbon monoxide. Chem Phys Lett 1996;260(3-4):471–475.

[14] Nasibulin AG, Pikhitsa PV, Jiang H, Kauppinen EI. Correlation between catalyst particle and single-walled carbon nanotube diameters. Carbon 2005;43(11):2251–2257.

[15] Gavillet J, Loiseau A, Journet C, Willaime F, Ducastelle F, Charlier JC. Root-growth mechanism for single-wall carbon nanotubes. Phys Rev Lett 2001;87(27):2755041–4.

[16] Fan X, Buczko R, Puretzky AA, Geohegan DB, Howe J, Pantelides S, Pennycook SJ. Nucleation of single-walled carbon nanotubes. Phys Rev Lett 2003;90(14):1455011–4.

[17] Raty JY, Gygi F, Galli G. Growth of carbon nanotubes on metal nanoparticles: A microscopic mechanism from ab initio molecular dynamics simulations. Phys Rev Lett 2005;95(9):0961031–4.

[18] Li L, Reich S, Robertson J. Modelling the nucleation and chirality selection of carbon nanotubes. J Nanosc Nanotech 2006;6(5):1290–1297.

[19] Reich S, Li L, Robertson J. Control the chirality of carbon nanotubes by epitaxial growth. Chem Phys Lett 2006;421(4-6):469–472.

[20] Ding F, Bolton K, Rosén A. Nucleation and growth of single-walled carbon nanotubes: A molecular dynamics study. J Phys Chem B 2004;108(45):17369–17377.

[21] Reich S, Li L, Robertson J. Epitaxial growth of carbon caps on Ni for chiral selectivity. Phys Stat Sol(b) 2006;243(13):3494–3499.

[22] Hofmann S, Csányi G, Ferrari AC, Payne MC, Robertson J. Surface diffusion: the low activation energy path for nanotube growth. Phys Rev Lett 2005;95(3):0361011–4.

[23] Shin Y, Hong S. Carbon diffusion around the edge region of nickel nanoparticles. Appl Phys Lett 2008;92(4):0431031-3.

[24] Hofmann S, Sharma R, Ducati C, Du G, Mattevi C, Cepek C, et al. In situ observations of catalyst dynamics during surface-bound carbon nanotube nucleation. Nano Lett 2007;7(3):602–608.

[25] Smalley RE, Li Y, Moore VC, Price BK, Colorado R, Schmidt HK Jr, et al. Single wall carbon nanotube amplification: En route to a type-specific growth mechanism. J Am Chem Soc 2006;128(49):15824–15829.

[26] Wang Y, Kim MJ, Shan H, Kittrell C, Fan H, Ericson LM, et al. Continued growth of single-walled carbon nanotubes. Nano Lett 2005;5(6):997–1002.

[27] Zhu W, Rosén A, Bolton K. Changes in single-walled carbon nanotube chirality during growth and regrowth. J Chem Phys 2008;128(12):1247081–6.

[28] Börjesson A, Zhu W, Amara H, Bichara C, Bolton K. Computational studies of metal-carbon nanotube interfaces for regrowth and electronic transport. Nano Lett 2009; accepted.

[29] Kresse G, Furthmüller J. Efficient iterative schemes for ab initio total-energy calculations using a plane-wave basis set. Phys Rev B 1996;54(16):11169–11186.

[30] Kresse G, Furthmüller J. Efficiency of ab-initio total energy calculations for metals and semiconductors using a plane-wave basis set. Comput Mater Sci 1996;6(1):15–50.

[31] Perdew JP, Chevary JA, Vosko SH, Jackson KA, Pederson MR, Singh DJ, Fiolhais C. Atoms, molecules, solids, and surfaces: applications of the generalized gradient approximation for exchange and correlation. Phys Rev B 1992;46(11):6671–6687.

[32] Larsson P, Larsson JA, Ahuja R, Ding F, Yakobson BI, Duan H, Rosén A, Bolton K. Calculating carbon nanotube-catalyst adhesion strengths. Phys Rev B 2007;75(11):1154191-6.

[33] Amara H, Bichara C, Ducastelle F. Formation of carbon nanostructures on nickel surfaces: A tight-binding grand canonical Monte Carlo study. Phys Rev B 2006;73(11):1134041–4.

[34] Frenkel D, Smit B. Molecular simulation: From algorithms to applications. London, UK: Oxford university press. 1997.

[35] Zhang QM, Wells JC, Gong XG, Zhang Z. Adsorption of a carbon atom on the Ni38 magic cluster and three low-index nickel surfaces: A comparative first-principles study. Phys Rev B 2004;69(20):2054131–7.

[36] Amara H, Bichara C, Ducastelle F. Understanding the nucleation mechanisms of carbon nanotubes in catalytic chemical vapor deposition. Phys Rev Lett 2008;100(5):0561051–4.

[37] Abild-Pedersen F, Nørskov JK, Rostup-Nielsen JR, Sehested J, Helveg S. Mechanisms for catalytic carbon nanofiber growth studied by ab initio density functional theory calculations. Phys Rev B 2006;73(11):11541901-13.

[38] Kanzow H, Ding A. Formation mechanism of single-wall carbon nanotubes on liquid-metal particles. Phys Rev B 1999;60(15):11180–11186.

[39] Bolton K, Ding F, Rosén A. Atomistic simulations of catalyzed carbon nanotube growth. J Nanosci Nanotechnol 2006;6(5):1211–1224.

[40] Zhang Y, Li Y, Kim W, Wang D, Dai H. Imaging as-grown single-walled carbon nanotubes originated from isolated catalytic nanoparticles. Appl Phys A 2002;74(3):325–328.

[41] Lee YH, Kim SG, Tománek D. Catalytic growth of single-wall carbon nanotubes: An ab initio study. Phys Rev Lett 1997;78(12):2393–2396.

[42] Baletto F, Ferrando R. Structural properties of nanoclusters: Energetic, thermodynamic, and kinetic effects. Rev Mod Phys 2005;77(1):371–423.

[43] Futschek T, Hafner J, Marsman M. Stable structural and magnetic isomers of small transition-metal clusters from the Ni group: an ab initio density-functional study. J Phys: Condens Matter 2006;18(42):9703–9748.

[44] Ding F, Larsson P, Larsson JA, Ahuja R, Duan H, Rosén A, Bolton K. The importance of strong carbon-metal adhesion for catalytic nucleation of single-walled carbon nanotubes. Nano Lett 2008;8(2):463–468.

[45] Qi Y, Çağin T, Johnson WL, Goddard III WA. Melting and crystallization in Ni nanoclusters: the mesoscale regime. J Chem Phys 2001;115(1):385–394.

[46] Amama PB, Pint CL, McJilton L, Kim SM, Stach EA, Murray PT, Hauge RH, Maruyama

B. Role of water in super growth of single-walled carbon nanotube carpets. Nano Lett 2009;9(1):44-49.

Figure Captions

Fig. 1 (Color online) Structures, together with their total energies, E_{tot}, relevant to the formation of (10,0) and (5,5) SWNT caps on a Ni_{55} cluster.

Fig. 2(Color online) (10,0) SWNT cap and fullerene cage structures attached to a Ni atom or Ni_{10} cluster. Total energies, E_{tot}, are given for each structure.

Fig. 3 (Color online) Total energies (upper panel) and Ni cluster diameters (lower panel) for the (5,5) and (10,0) SWNTs and C_{80} fullerenes on different sized Ni clusters. Energies for C_{80}/Ni_{201} systems were not determined due to the computational expense.

Fig. 4(Color online) Energy histograms from TBMC simulations at 1000K for SWNT/Ni_N (solid curves) and C_{80}/Ni_N (dashed curves), where N = 10, 25, and 55.

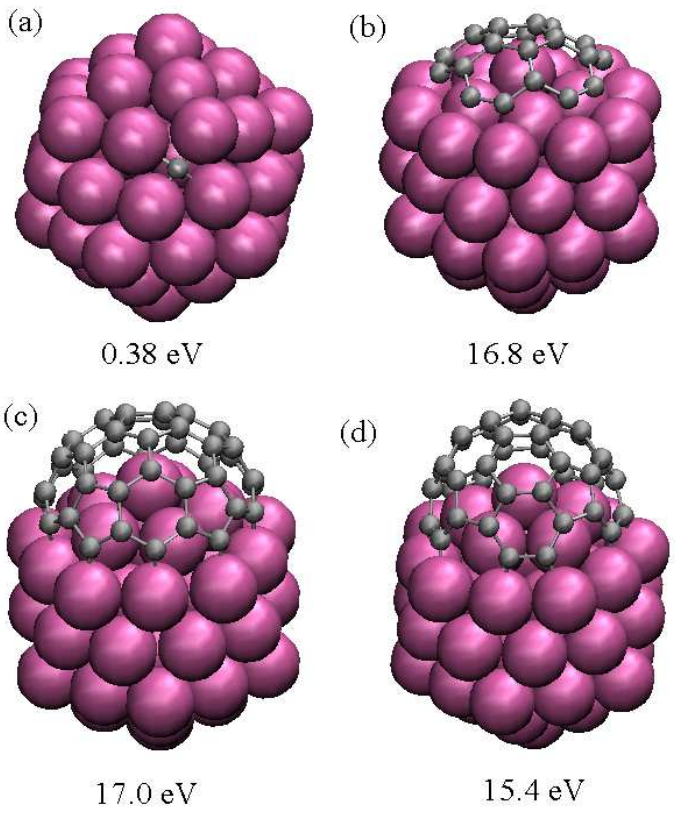

Figure 1. Zhu, Börjesson, Rosén, XXX, and Bolton;

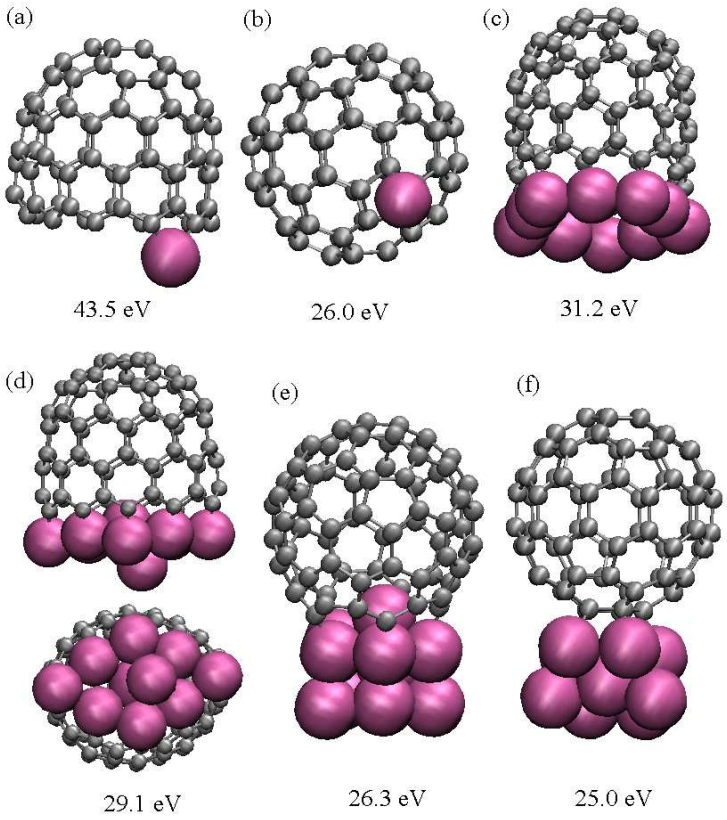

Figure 2. Zhu, Börjesson, Rosén, XXX, and Bolton;

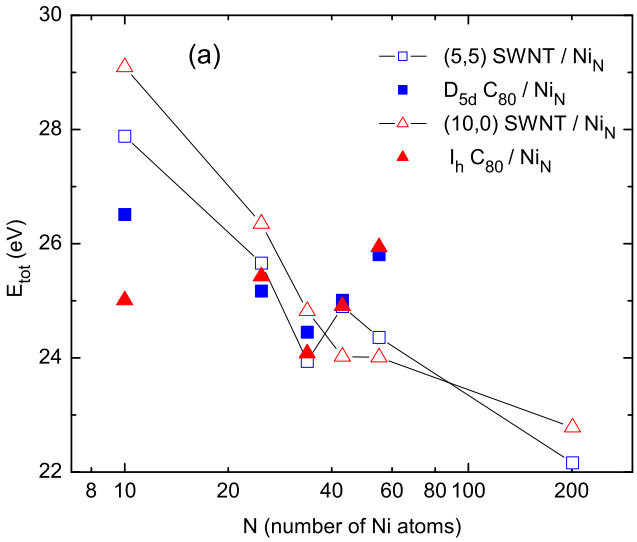

Figure 3(a). Zhu, Börjesson, Rosén, XXX, and Bolton;

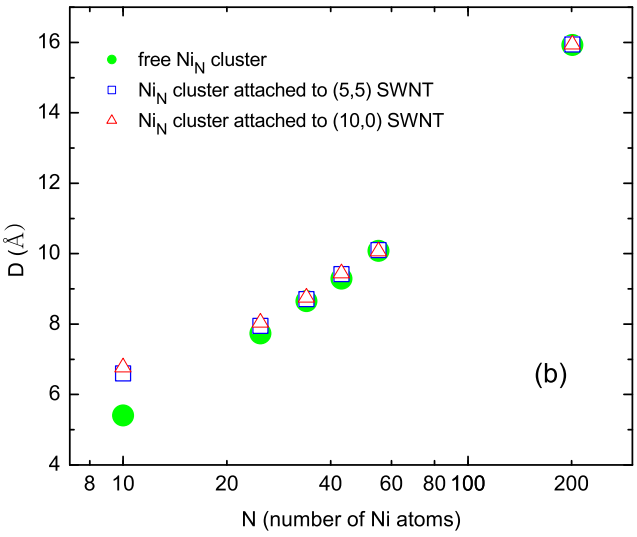

Figure 3(b). Zhu, Börjesson, Rosén, XXX, and Bolton;

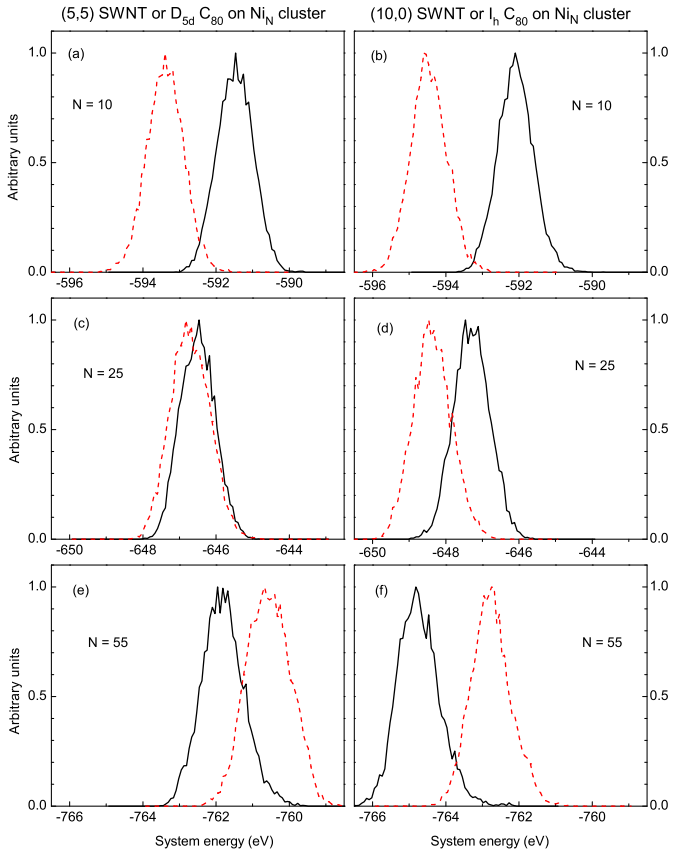

Figure 4. Zhu, Börjesson, Rosén, XXX, and Bolton;